JCI INSIGHT

Cullin-3 mutation causes arterial stiffness and hypertension through a vascular smooth muscle mechanism

Larry N. Agbor,[1] Stella-Rita C. Ibeawuchi,[1] Chunyan Hu,[1] Jing Wu,[1] Deborah R. Davis,[1] Henry L. Keen,[1] Frederick W. Quelle,[1] and Curt D. Sigmund[1,2]

[1]Department of Pharmacology and [2]UIHC for Hypertension Research, Roy J. and Lucille A. Carver College of Medicine, University of Iowa, Iowa City, Iowa, USA.

Cullin-3 (*CUL3*) mutations (*CUL3Δ9*) were previously identified in hypertensive patients with pseudohypoaldosteronism type-II (PHAII), but the mechanism causing hypertension and whether this is driven by renal tubular or extratubular mechanisms remains unknown. We report that selective expression of CUL3Δ9 in smooth muscle acts by interfering with expression and function of endogenous CUL3, resulting in impaired turnover of the CUL3 substrate RhoA, increased RhoA activity, and augmented RhoA/Rho kinase signaling. This caused vascular dysfunction and increased arterial pressure under baseline conditions and a marked increase in arterial pressure, collagen deposition, and vascular stiffness in response to a subpressor dose of angiotensin II, which did not cause hypertension in control mice. Inhibition of total cullin activity increased the level of CUL3 substrates cyclin E and RhoA, and expression of CUL3Δ9 decreased the level of the active form of endogenous CUL3 in human aortic smooth muscle cells. These data indicate that selective expression of the *Cul3Δ9* mutation in vascular smooth muscle phenocopies the hypertension observed in *Cul3Δ9* human subjects and suggest that mutations in CUL3 cause human hypertension in part through a mechanism involving smooth muscle dysfunction initiated by a loss of CUL3-mediated degradation of RhoA.

Introduction

Hypertension must be aggressively treated to minimize the risk of cardiovascular events and death, as it is a risk factor for cardiovascular mortalities from events such as stroke and heart failure. There is a continuing need to identify and elucidate novel pathways that regulate blood pressure (BP) in order to develop novel therapies. Emerging evidence suggests that cullin-3 (CUL3) plays an important role controlling arterial BP (1, 2). CUL3 is a critical subunit of the CUL3-Ring-Ligase (CRL3) ubiquitin ligase complex, for which CUL3 acts as a molecular scaffold linking the E3 ubiquitin ligase Rbx1 with adaptors carrying protein substrates. Proteins that are ubiquitinated by active CRL3 complexes become targets for proteasomal degradation (3).

Mutations in *CUL3* were identified by exome sequencing in pseudohypoaldosteronism type II (PHAII), a monogenetic form of human hypertension (2). The mutations are located in the splice donor and acceptor sites surrounding exon 9 and cause exon skipping of exon 9 through missplicing of *CUL3* mRNA. This results in an in-frame deletion of 57 amino acids internal to CUL3. Evidence that the mutant protein (termed CUL3Δ9) has dominant-negative activity includes that (a) CUL3Δ9 supports impaired ubiquitin ligase activity toward normal substrates, (b) CUL3Δ9 exhibits enhanced binding to substrate adaptors and promotes their degradation, and (c) CUL3Δ9 may form inhibitory and unstable heterodimers with wild-type CUL3 (CUL3WT) (4–6).

With-no-lysine serine-threonine kinase 4 (WNK4) is a CRL3 substrate, and mutations in CUL3 and KLHL3 (the substrate recognition protein delivering WNK4 to CUL3) impair the ability of the CRL3 complex to degrade WNK4 in the kidney (7, 8). WNK4 is a known regulator of ion transporters in the kidney, and mutations in WNK4 cause hypertension (9). Both of these observations led investigators to primarily focus on a renal tubular mechanism for hypertension associated with CUL3Δ9 mutations. However, other evidence argues that extratubular mechanisms, particularly vascular mechanisms, may also play an important role in hypertension caused by CUL3 mutations. For example, despite abnormalities in electrolyte han-
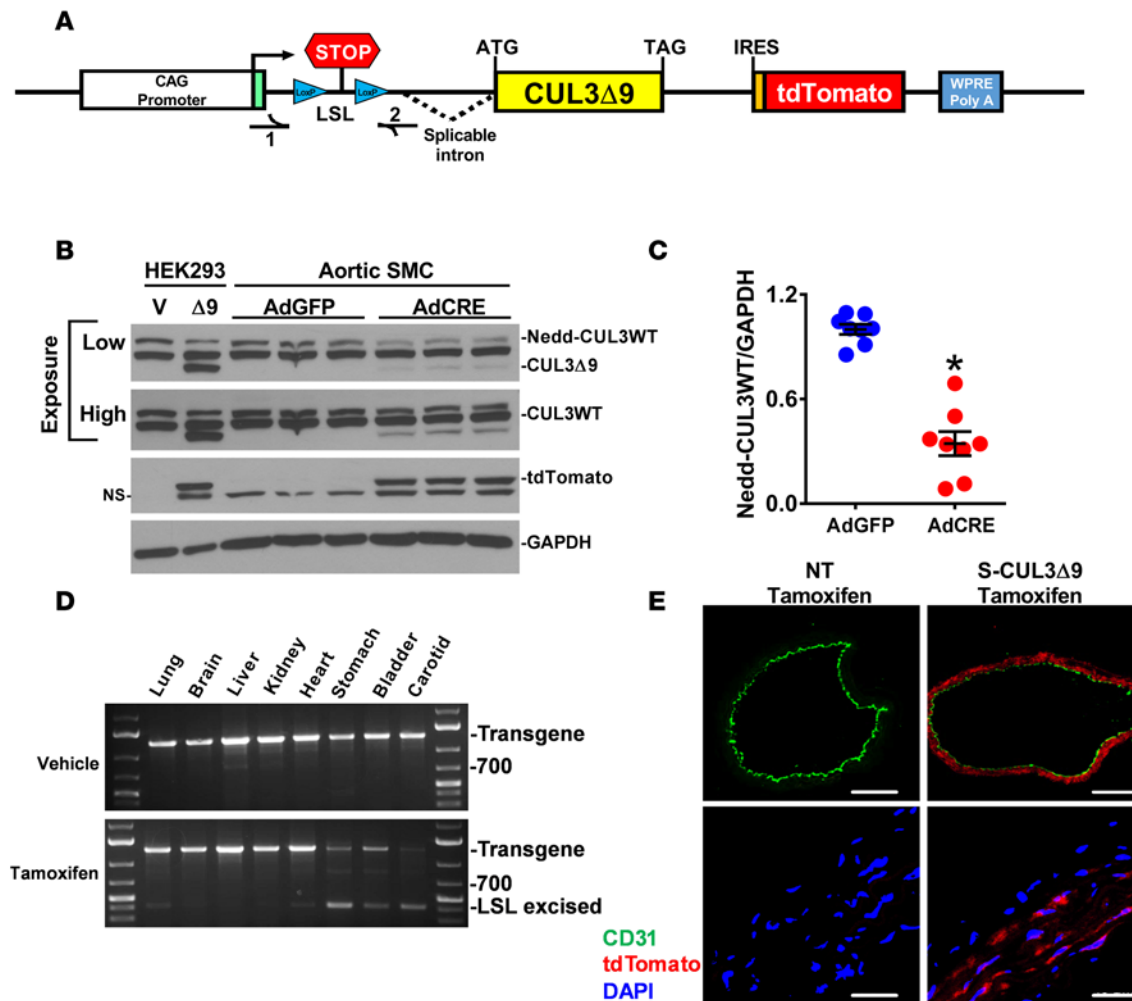
Figure 1. Smooth muscle–specific expression of CUL3Δ9. (**A**) Schematic of construct used to generate inducible cell-specific *CUL3Δ9* transgenic mice. *CUL3Δ9* cDNA was generated by overlap splice extension PCR and cloned into a vector, which we previously described (26, 30). (**B**) Aortic smooth muscle cells (SMC) were isolated from *CUL3Δ9* transgenic mice and infected with adenovirus expressing either Cre recombinase (AdCRE) or GFP (AdGFP). The first two control lanes are HEK293 cells transfected with either empty vector (V) or *CUL3Δ9* construct (Δ9) to provide a marker for the position of the CUL3Δ9 protein band. A low and high exposure of the same blot are shown to show the decrease in neddylated CUL3WT (top) and the expression of CUL3Δ9 (bottom). This is a representative of 4 independent experiments. (**C**) Quantification of neddylated CUL3WT (Nedd-CUL3WT) (*n* = 8). Error bars represent the mean ± SEM. *$P < 0.001$ by 2-tailed *t* test. (**D**) PCR analysis of genomic DNA providing evidence of Cre-mediated excision in smooth muscle–enriched tissues from vehicle- or tamoxifen-treated S-CUL3Δ9 mice. The positions of the transgene and recombined transgene after excision of the lox-STOP-lox (LSL excised) sequence are indicated. (**E**) Aortic sections from tamoxifen-treated nontransgenic (NT) and S-CUL3Δ9 mice were immunostained for the endothelial marker CD31 (green), stained with DAPI (blue), and were visualized for intrinsic fluorescence of tdTomato reporter (red). Original magnification, ×10; scale bar: 200 μm (top). Original magnification, ×60; scale bar: 10 μm (bottom). NS, nonspecific band; V, vehicle; NT, nontransgenic mice.

dling, kidney-specific deletion of CUL3 results in hypotension, not hypertension (5). Conversely, expression of the human hypertension-causing PPARγ P467L mutation in smooth muscle causes hypertension in mice consequent to a loss of expression of CUL3 protein (1, 10). Direct effects on vascular function are also suggested by the observation that expression of Cul3Δ9 in all mouse tissues results in increased arterial stiffness (6). Thus, the mechanism whereby CUL3 mutations cause hypertension and the role of vascular smooth muscle CUL3 are not clear.

We tested the hypothesis that selective expression of CUL3Δ9 in vascular smooth muscle can recapitulate hypertension observed in patients bearing the mutation. We show that smooth muscle–specific expression of CUL3Δ9 interferes with endogenous CUL3WT, causes vascular dysfunction and hypertension, abrogates aortic compliance, impairs the vasodilator effects of NO, and augments the pressor response to angiotensin II (Ang II). These studies (a) unravel a vascular component that contributes to hypertension in patients with CUL3 mutations and (b) validate the CUL3-RhoA/Rho kinase pathway as an important regulator of arterial BP.
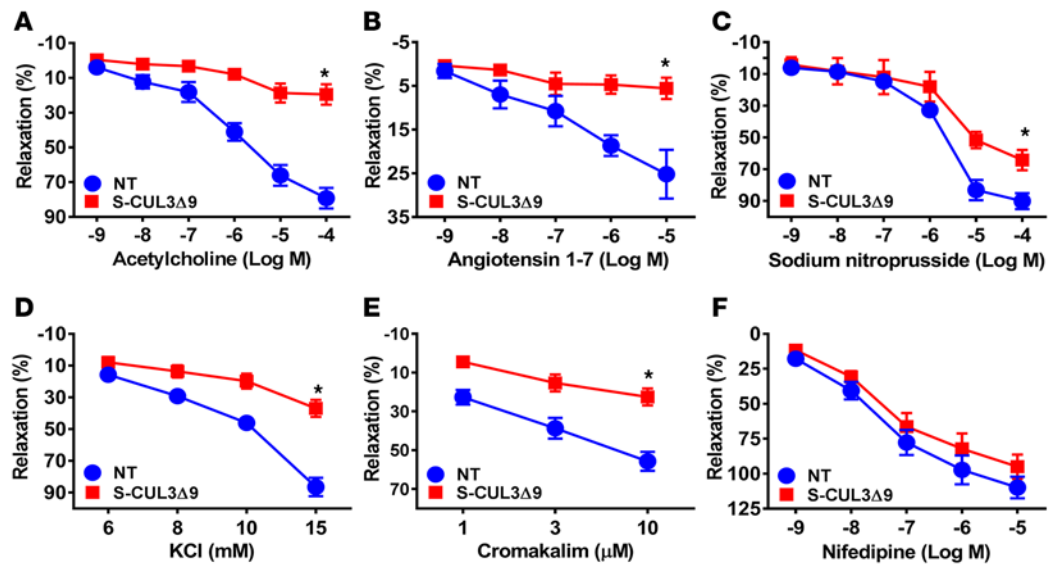
Figure 2. Vasodilation in the basilar arteries from S-CUL3Δ9 mice. Dose-dependent relaxation was measured in basilar arteries from nontransgenic (NT) and S-CUL3Δ9 mice. Arteries were pressurized to 60 mmHg and precontracted with the thromboxane A2 mimetic (U46619) to 30% internal diameter. Dose-dependent relaxation in response to acetylcholine (**A**, n = 5), angiotensin 1–7 (**B**, n = 4–6), sodium nitroprusside (**C**, n = 3–4), low-dose potassium chloride (KCl) (**D**, n = 7), cromakalim (**E**, n = 7), and nifedipine (**F**, n = 7) was assessed. Error bars represent the mean ± SEM. *P < 0.05 by 2-way repeated-measure ANOVA.

Results

We generated transgenic mice designed to inducibly express CUL3Δ9 and the tdTomato reporter in response to activation of Cre recombinase induced by tamoxifen (Figure 1A). Expression of CUL3Δ9 and tdTomato was first examined in primary aortic smooth muscle cells (SMC) cultured from CUL3Δ9 transgenic mice. Activation of the transgene by infection with an adenovirus encoding Cre recombinase resulted in robust expression of tdTomato and modest expression of CUL3Δ9 proteins (Figure 1B). Interestingly, coincident with CUL3Δ9 expression was a very reproducible decrease in the level of endogenous neddylated CUL3WT, the active form of the protein, suggesting impaired CUL3 activity (Figure 1C). To examine the physiological significance of the CUL3Δ9 mutation in vivo, we bred *CUL3Δ9* transgenic mice with mice expressing tamoxifen-inducible CRE[ERT2] under control of the smooth muscle myosin heavy chain promoter to generate the S-CUL3Δ9 mouse model. PCR analysis of tissue genomic DNA from vehicle- and tamoxifen-treated mice showed Cre-dependent recombination in smooth muscle–enriched tissues, such as carotid artery, stomach, bladder, and, to a lesser extent, lung and heart, with little evidence of recombination in brain, liver, and kidney (Figure 1D). Strongly positive tdTomato reporter staining was detected in the medial smooth muscle layer of tamoxifen-treated S-CUL3Δ9 aortas (Figure 1E). There was no staining in smooth muscle or endothelium in aortas from tamoxifen-treated nontransgenic (NT) mice or in the endothelium in aortas from tamoxifen-treated S-CUL3Δ9 mice. These data confirm smooth muscle selective expression of the *CUL3Δ9* transgene in the blood vessel.

The basilar artery is a cerebral artery with particular sensitivity to interference with PPARγ, an upstream regulator of CUL3 (11). Thus, we first examined vascular function in the basilar arteries in S-CUL3Δ9 and NT mice after 4 weeks of transgene expression. This vessel from S-CUL3Δ9 mice exhibited severely impaired vasodilation in response to the endothelium-dependent agonists acetylcholine (ACh) (Figure 2A) and angiotensin 1–7 (Figure 2B). Inhibition of NO synthase by L-NAME abolished vasodilation to ACh, suggesting this relaxation was predominantly NO dependent (Supplemental Figure 1A; supplemental material available online with this article; doi:10.1172/jci.insight.91015DS1). The vessel also exhibited modestly impaired vasodilation to the endothelium-independent NO donor SNP (Figure 2C). Vasodilation to low-dose KCl and an ATP-sensitive K-channel activator was similarly impaired (Figure 2, D and E), but vasodilation to the calcium channel blocker nifedipine was normal (Figure 2F), indicating some specificity in the mechanism causing impairment. Importantly, vasodilation to both ACh and SNP
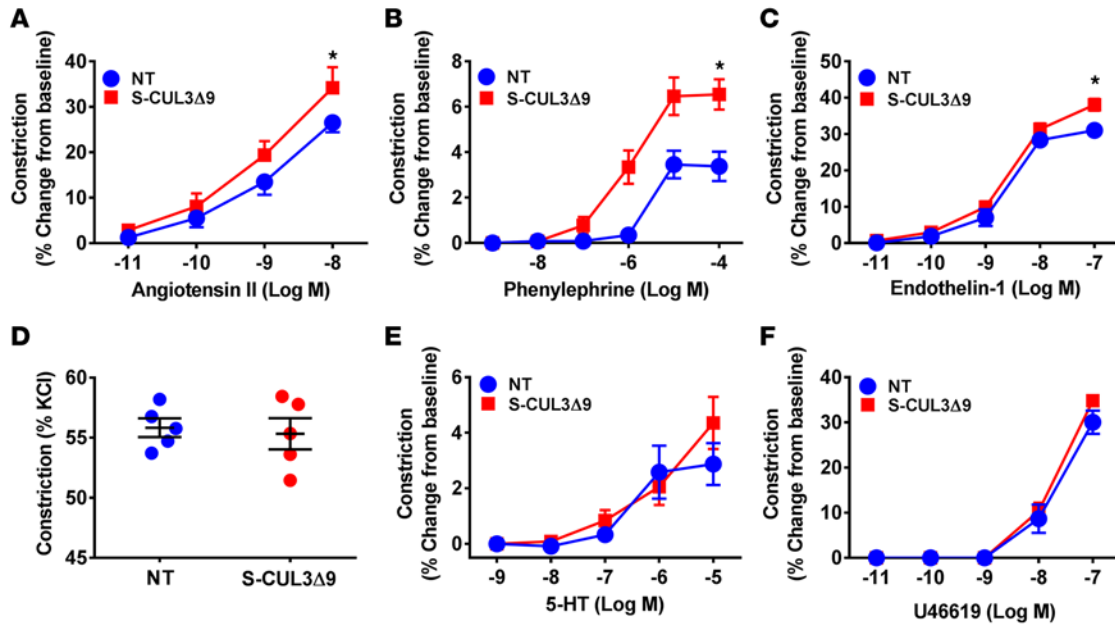
Figure 3. Vasoconstriction in the basilar arteries from S-CUL3Δ9 mice. Dose-dependent vasoconstriction of the basilar arteries from nontransgenic (NT) and S-CUL3Δ9 mice. Arteries were equilibrated for 30 minutes at 60 mmHg under no-flow conditions, and vasoconstriction responses to angiotensin II (**A**, $n = 7$), phenylephrine (**B**, $n = 7$), endothelin-1 (**C**, $n = 7$–10), potassium chloride (**D**, $n = 3$–5), 5-hydroxytryptamine hydrochloride (5-HT or serotonin) (**E**, $n = 7$), and the thromboxane A2 mimetic (U46619) (**F**, $n = 3$) were assessed. Error bars represent the mean ± SEM. *$P < 0.05$ by 2-way repeated-measure ANOVA.

was normal in the basilar arteries from tamoxifen-treated ROSA22[tdTomato] reporter mice bred to the same Cre recombinase driver (Supplemental Figure 1, B and C), indicating the impaired vasodilation was not due to overexpression of the tdTomato reporter embedded in the *CUL3Δ9* transgene. Contractile responses were also augmented in response to some (Figure 3, A–C), but not all, agonists (Figure 3, D–F). There were no changes in external diameter, lumen diameter, and wall thickness in the basilar arteries 4 weeks after tamoxifen (Supplemental Figure 2). These data suggest that selective expression of CUL3Δ9 in smooth muscle causes vascular dysfunction.

Consistent with results from the basilar artery, impaired relaxation in response to ACh was also evident in the aorta, a conduit artery of sufficient mass to facilitate studies of molecular mechanisms (Figure 4A). The impaired ACh response occurred without a change in the level of total and phosphorylated endothelial NO synthase, suggesting the impairment is caused by an alternative mechanism (Supplemental Figure 3). There was reduced expression of both neddylated and unneddylated CUL3WT in aortas (Figure 4, B and C). Interestingly, despite abundant expression of the embedded tdTomato reporter protein (and abundant tdTomato and CUL3Δ9 mRNA, data not shown), we could not detect CUL3Δ9 protein (Figure 4B). Previously, CUL3Δ9 was reported to form unstable heterodimers with CUL3WT (4), suggesting the possibility that the decrease in endogenous CUL3WT and inability to detect CUL3Δ9 in mouse aorta may result from rapidly degraded CUL3Δ9/CUL3WT heterodimers. Consistent with a reduction in active CUL3WT, expression of total RhoA protein, a CUL3 substrate, was increased in the aortas of S-CUL3Δ9 mice (Figure 4, B and C). Whereas there was no difference in the level of the active form of RhoA (RhoA-GTP) at baseline, 5-hydroxytryptamine hydrochloride (5-HT) stimulation increased RhoA-GTP to a greater degree in S-CUL3Δ9 aortas than NT aortas (Figure 4D). The 5-HT–induced increase in RhoA-GTP was similar to that caused by the direct RhoA activator, CN03 (Figure 4E). We conclude that impairing CUL3 activity in vascular smooth muscle results in increased RhoA levels, which provide an increased pool of RhoA that can be activated in response to signals from the cell surface.

Increased active RhoA suggests an increase in Rho kinase (ROCK) activity. Consistent with this, the phosphorylated form of myosin phosphatase target subunit 1 (MYPT1), a ROCK substrate, was elevated in aortas from S-CUL3Δ9 mice (Figure 5A). Therefore, we assessed whether the impairment in vasodilation observed in the basilar arteries and aortas in S-CUL3Δ9 mice occurred through a ROCK-dependent mechanism. Vasodilation to ACh was impaired in aortas (Figure 5B) and basilar arteries (Figure 5C) in this
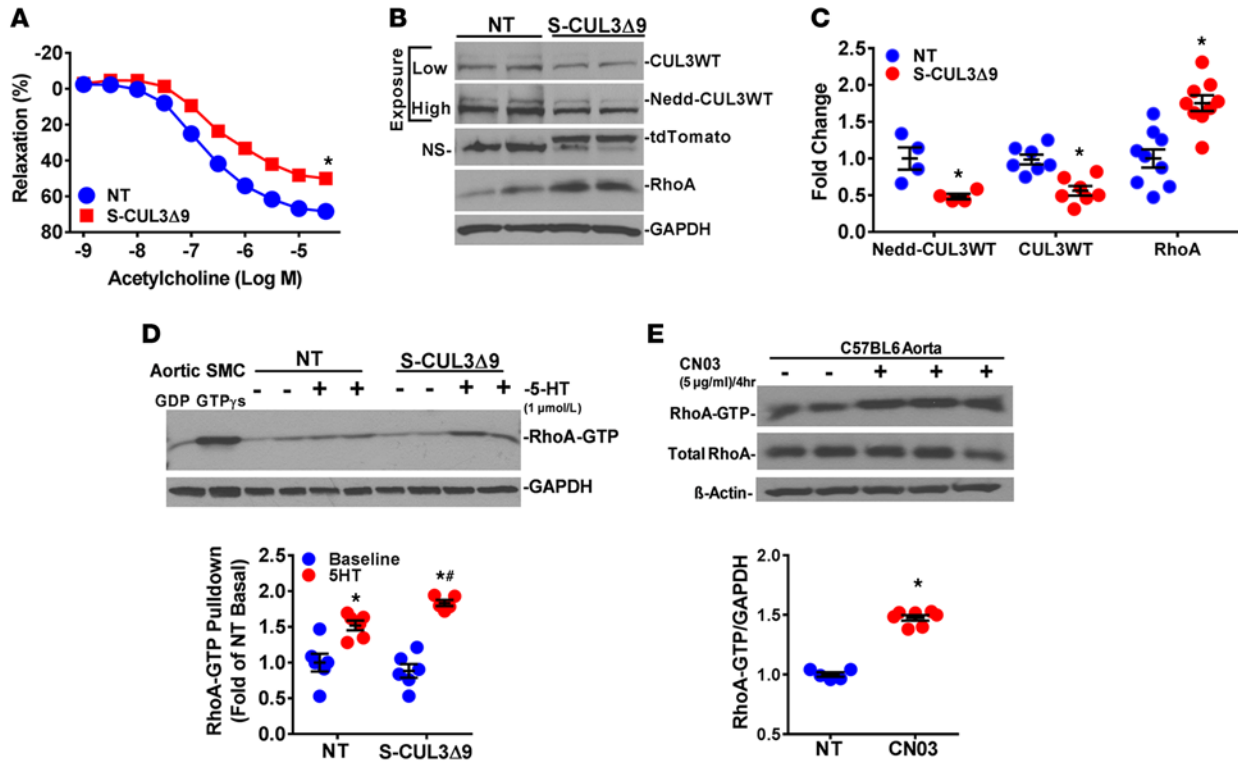
Figure 4. S-CUL3Δ9 aortas exhibit elevated RhoA. (**A**) Vasorelaxation in response to acetylcholine in aortas from nontransgenic (NT) and S-CUL3Δ9 mice (*n* = 14–16). 3- to 4-mm aortic sections were equilibrated at 0.5 *g* for 45 minutes in an organ bath, preconstricted with PGF$_{2\alpha}$ to 45%–50% of maximal response to U46619, and the dose-response to ACh was assessed. *$P < 0.05$, S-CUL3Δ9 vs. NT by 2-way repeated-measure ANOVA. (**B**) Expression of the indicated proteins in aortas from NT and S-CUL3Δ9 mice. (**C**) Quantification of neddylated CUL3WT, unneddylated CUL3WT, and RhoA in aortas from NT and S-CUL3Δ9 mice. *n* = 4–9/genotype. *$P < 0.05$, S-CUL3Δ9 vs. NT by 2-tailed *t* test. (**D**) Levels of active RhoA-GTP from aortic rings from NT and S-CUL3Δ9 mice using a pulldown assay. Aortas were equilibrated to 0.5 *g* tension, with or without serotonin (5-HT) (1 μmol/l, 5 minutes) as indicated. The level of RhoA-GTP was quantified. *n* = 5–6/genotype/treatment. *$P < 0.05$, 5-HT vs. baseline; #$P < 0.05$, 5-HT S-CUL3Δ9 vs. 5-HT NT by 1-way ANOVA. This is a representative of 3 independent experiments. (**E**) Levels of active RhoA-GTP from aortic rings from C57BL/6 mice using a pulldown assay. Aortic rings were incubated with the RhoA activator CN03 or saline (5 μg/ml, 4 hours). The level of RhoA-GTP was quantified (*n* = 5–7/treatment). Error bars represent mean ± SEM. *$P < 0.05$, CN03 vs. saline by Student's *t* test. This is a representative of 2 independent experiments. NS, nonspecific bands; SMC, smooth muscle cell; GDP, guanosine diphosphate; GTPγs, guanosine triphosphate γ S.

independent cohort of S-CUL3Δ9 mice. Preincubation with the ROCK inhibitor Y-27632 restored ACh relaxation in both vessels. The Y-27632–sensitive impairment in ACh is likely to reflect increased RhoA activity, since Y-27632 also restored the ACh response in the basilar arteries impaired by CN03-mediated RhoA activation (Figure 5D). These data suggest the impairment in vasodilatation caused by expression of CUL3Δ9 in smooth muscle is a result of increased RhoA-induced ROCK activity.

To assess if these results have relevance in human SMC, primary human aortic SMC (HASMC) were treated with the Nedd8-activating enzyme inhibitor, MLN4924. This treatment completely ablated neddylated CUL3 and increased RhoA and cyclin E proteins, two bona fide CUL3 substrates (Figure 6A). The level of RhoA induction was similar to that observed in primary mouse aortic SMC in response to CUL3Δ9 and in aortas from S-CUL39 mice. Moreover, infection of HASMC with an adenovirus expressing CUL3Δ9 decreased the level of active neddylated CUL3 (Figure 6B). There was a significant increase in the level of unneddylated CUL3 in HASMC transduced with adenovirus expressing CUL3WT, although there was no significant change in the level of neddylated CUL3, suggesting tight control over the level of active CUL3.

We next measured arterial BP by radiotelemetry to assess if expression of CUL3Δ9 in smooth muscle can cause hypertension. Normal circadian rhythm was preserved, but systolic BP (SBP) was significantly increased in S-CUL3Δ9 mice 2 weeks after tamoxifen treatment (Figure 7A). Interestingly, the increase in SBP was only significant during daytime hours, a result that was replicated 4 weeks after tamoxifen treatment (Supplemental Figure 4A). There was no significant change in mean and diastolic BP (data not shown). Consistent with this, there was a trend toward increased pulse pressure in S-CUL3Δ9 mice at 2 and
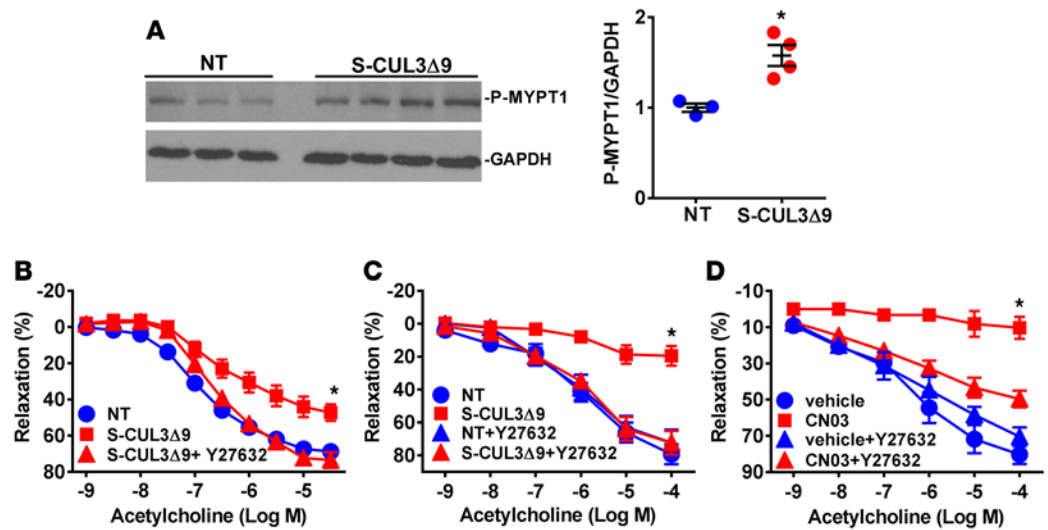
Figure 5. S-CUL3Δ9 aortas exhibit elevated ROCK activity. (**A**) Western blot and quantification of the phosphorylated form of myosin phosphatase target subunit 1 (MYPT1) from nontransgenic (NT) and S-CUL3Δ9 aortas (*n* = 3–4/genotype). *$P < 0.05$, S-CUL3Δ9 vs. NT by Student's *t* test. (**B** and **C**) Effect of the Rho-kinase inhibitor, Y-27632 (1 μmol/l, 30 minutes), on acetylcholine-mediated relaxation in aortas (**B**, *n* = 4–6) and basilar arteries (**C**, *n* = 5) from S-CUL3Δ9 mice compared with NT mice. Error bars represent the mean ± SEM. *$P < 0.05$. S-CUL39 vs. all other curves by 2-way repeated-measure ANOVA. (**D**) Effect of the Rho-kinase inhibitor, Y-27632 (1 μmol/l, 30 minutes), on acetylcholine-mediated relaxation in basilar arteries treated with CN03. *n* = 3/genotype or treatment. Error bars represent the mean ± SEM. *$P < 0.05$, CN03 vs. all other curves by 2-way repeated-measure ANOVA.

4 weeks (Figure 7B and Supplemental Figure 4B). There were no differences in heart rate and activity (Supplemental Figure 4, C and D). Given the modest increase in BP, we asked if S-CUL3Δ9 mice were more susceptible to a hypertension-causing stimulus. To test this, we administered a dose of Ang II that does not significantly increase BP in control mice via osmotic minipumps. S-CUL3Δ9 mice were highly susceptible to the pressor response elicited by subcutaneous administration of subpressor Ang II (Figure 7C). Mean and diastolic BP were also significantly increased by Ang II in S-CUL3Δ9 mice (Supplemental Figure 5, A and B). There was no change in heart rate after Ang II (Figure 7D). Taken together, these data suggest that S-CUL3Δ9 mice exhibit isolated systolic hypertension and are sensitized to the pressor effect of Ang II.

Isolated systolic hypertension is often an indicator of impaired arterial compliance or increased arterial stiffness (12). We therefore measured pulse wave velocity (PWV), an index of aortic stiffness, by Doppler ultrasound. PWV was significantly increased in S-CUL3Δ9 mice 4 weeks after tamoxifen (Figure 8A), a phenotype that remained at 8 weeks (Supplemental Figure 5C). We also measured aortic compliance by examining the pressure-diameter and stress-strain relationships. There was no significant difference in aortic compliance at baseline, but administration of subpressor Ang II led to a downward shift of the pressure-diameter relationship and a leftward shift of the stress-strain curve indicative of aortic stiffening (Figure 8, B and C, and Supplemental Figure 5D). Hydroxyproline, a measurement of aortic collagen content (Figure 8D), and total protein (Supplemental Figure 5E) were significantly increased in S-CUL3Δ9 aortas following Ang II administration. The increase in hydroxyproline was consistent with increased adventitial collagen deposition, as shown by Masson's trichrome staining (Figure 8E and Supplemental Figure 5F). Thus, the expression of CUL3Δ9 in smooth muscle impairs arterial compliance and predisposes to Ang II–induced aortic stiffening.

Discussion

Several lines of evidence led us to focus on the role of smooth muscle CUL3 in BP control. PHAII patients with dominant mutations in *CUL3* (*CUL3Δ9*) and mutations in the gene encoding the CUL3 substrate recognition protein *KLHL3* exhibit severe early-onset hypertension (2). These mutations could affect BP by impairing the ability of CUL3 to degrade WNK kinases, leading to increased activity of the renal sodium chloride cotransporter (7). However, expression of dominant-negative PPARγ specifically in smooth muscle in mice (S-P467L) causes a loss of CUL3 protein in vascular tissue, which was associated with impaired turnover
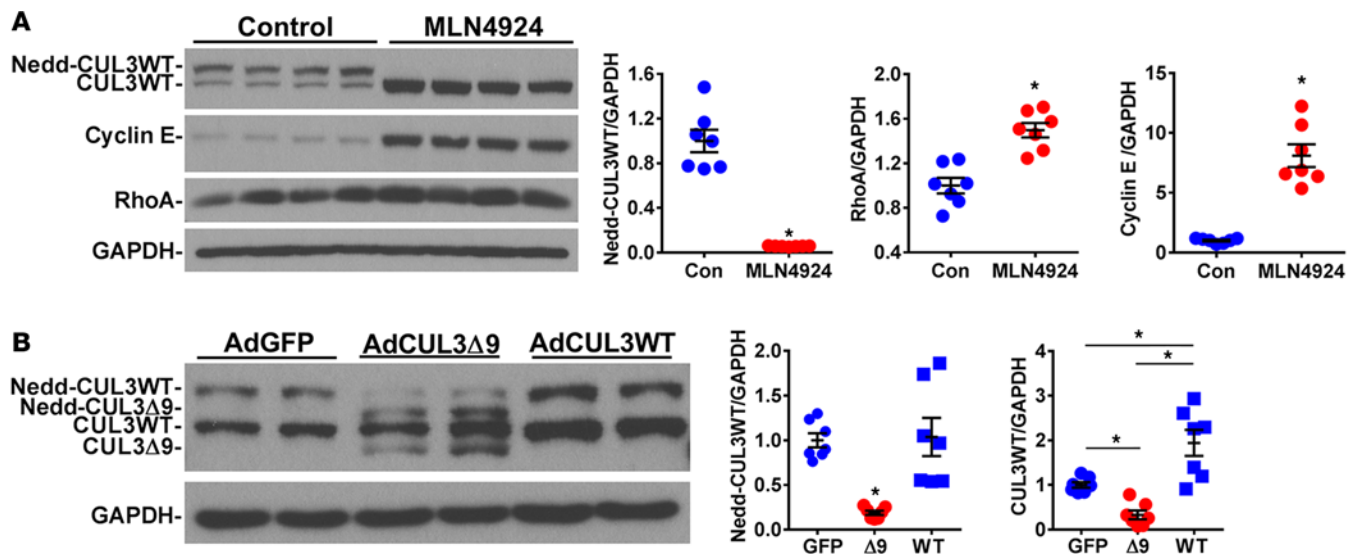
Figure 6. Role of cullin-3 in primary human aortic smooth muscle cells. (A) Primary human aortic smooth muscle cells were cultured to 90% confluency. Expression of the indicated proteins in primary human aortic smooth muscle cells treated with the pan-cullin inhibitor, MLN4924 (1 μmol/l), for 24 hours. Quantification of independent samples is shown. $n = 7$. Error bars represent mean ± SEM. *$P < 0.05$, control vs. MLN4924 by Student's t test. This is a representative of 2 independent experiments. **(B)** Expression of the indicated proteins in primary human smooth muscle cells after infection with adenovirus expressing GFP (AdGFP) or CUL3Δ9 (AdCUL3Δ9) or CUL3WT (AdCUL3WT) for 72 hours. Quantification of independent samples is shown. $n = 7$. Error bars represent mean ± SEM. *$P < 0.05$ by 1-way ANOVA. This is a representative of 2 independent experiments. Con, control; WT, CUL3WT; Δ9, CUL3Δ9.

and degradation of RhoA, elevated Rho kinase signaling, vascular dysfunction, and hypertension (1). While the global loss of CUL3 is embryonically lethal in mice (13), nephron-specific deletion of CUL3 results in hypotension (5), suggesting that extratubular mechanisms could contribute to elevated BP in patients with mutant CUL3. Our data are consistent with this hypothesis and provide evidence supporting the concept that CUL3 directly regulates arterial BP through its activity in vascular smooth muscle, and its impaired function in smooth muscle contributes to the hypertension in patients with CUL3 mutations. Mechanistically, expression of the hypertension-causing CUL3Δ9 mutation impairs vascular function as a result of (a) compromised endogenous CUL3 activity resulting in decreased turnover of RhoA and elevated RhoA and ROCK activity, (b) impaired response to endothelial-derived NO-dependent relaxation, (c) enhanced agonist-induced vasocontraction, and (d) increased arterial stiffness and fibrosis that reduce arterial compliance, all of which cause hypertension and increased susceptibility to an agonist-induced hypertension.

The neddylation of cullin proteins, a process whereby nedd8 is conjugated to Lys-712 of CUL3, is necessary for CUL3 activation and substrate ubiquitination (14). Although CUL3Δ9 has been previously reported to undergo increased neddylation (5), we reported that neddylation of CUL3Δ9 is decreased compared with CUL3WT, and its interaction with the E3 ubiquitin ligase Rbx1 is also impaired (4). We have also reported that CUL3Δ9 forms an unstable heterodimer when complexed with CUL3WT. Thus, our finding herein that expression of CUL3Δ9 in vascular smooth muscle reduces the level of endogenous CUL3 and neddylated CUL3 is consistent with the formation of an unstable heterodimer and consequent degradation of the complex. This is indirectly supported by the observation that, despite abundant tdTomato reporter expression in medial aortic smooth muscle and abundant mRNA expression of CUL3Δ9 and tdTomato, we were unable to observe CUL3Δ9 protein in aortas from S-CUL3Δ9 mice.

Abnormalities in RhoA/ROCK regulation have been implicated in several cardiovascular diseases (15). The system serves as a molecular switch that regulates calcium sensitization in smooth muscle (16) and augments vasoconstriction to agonists (17). Knockdown of CUL3 or pharmacological blockade of total cullin activity increases RhoA protein expression (18, 19). Similarly, interference with endogenous CUL3 by CUL3Δ9 in smooth muscle enhanced total and active RhoA expression and phosphorylated MYPT1 in S-CUL3Δ9 aortas indicative of increased ROCK signaling. Increased ROCK signaling promotes a procontractile state, resulting in enhanced responses to G protein–coupled receptor agonists (17). Activation of ROCK also results in impaired relaxation of smooth muscle in response to endothelium-derived NO, without a change in the level of phospho-eNOS and total
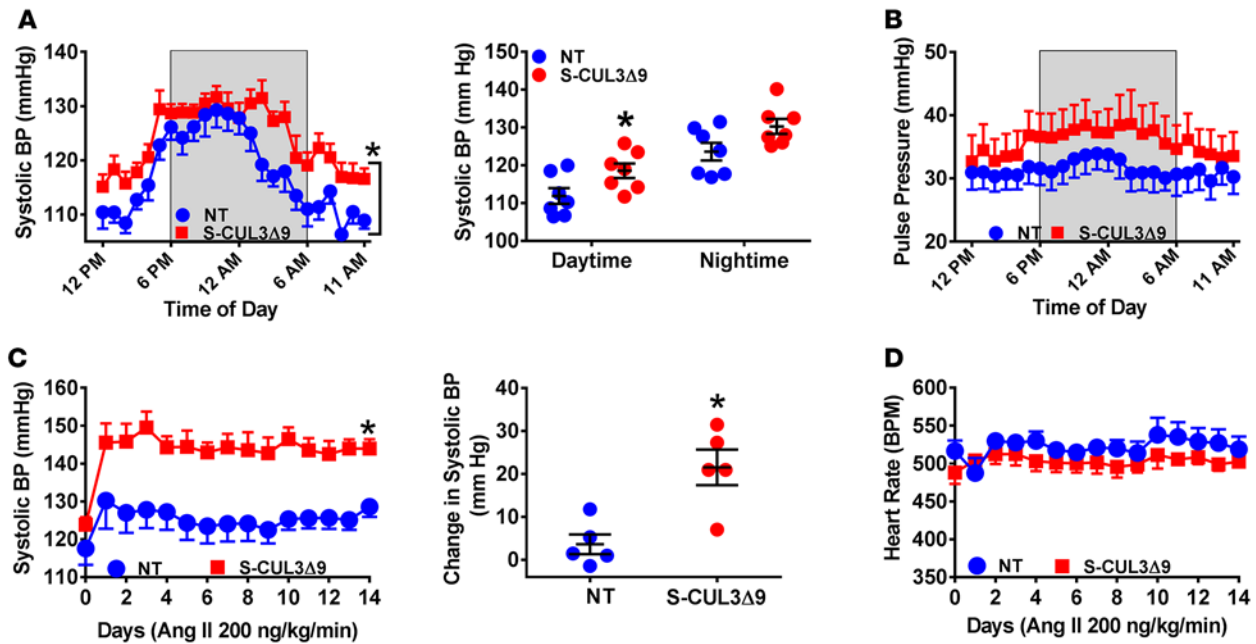
Figure 7. Blood pressure in S-CUL3Δ9 mice. (**A** and **B**) Systolic blood pressure (**A**) and pulse pressure (**B**) were measured continuously every 5 minutes for 10 seconds by radiotelemetry for 7 days, starting 2 weeks after tamoxifen in nontransgenic (NT) and S-CUL3Δ9 mice. The data are collapsed onto a single 24-hour-light/dark cycle. Shaded areas indicate the dark cycle. n = 6–7/genotype. *P < 0.05 S-CUL3Δ9 vs. NT by 2-way ANOVA with repeated measure-ments. (**C** and **D**) Effects of acute angiotensin II (Ang II) administration on systolic blood pressure (**C**) and heart rate (**D**) in NT and S-CUL3Δ9 mice, as measured by radiotelemetry. Mice were continuously administered Ang II (200 ng/kg/min) through an osmotic minipump for 14 days, and blood pressure was recorded by radiotelemetry as described. Day 1 indicates the start of Ang II infusion. n = 5/genotype. *P < 0.05 S-CUL3Δ9 vs. NT by 2-way ANOVA with repeated measurements.

eNOS, suggesting that endothelial function is preserved but smooth muscle is unresponsive. This is confirmed by (a) the impaired smooth muscle response to chemical activation of RhoA, which locks RhoA in its GTP-bound state, in vessels from normal mice, and (b) restoration of the response after ROCK blockade. That inhibition of cullin activity in primary HASMC results in increased RhoA expression implies that the CUL3-RhoA pathways is active in human SMC. It remains to be deter-mined if PHAII patients with mutations in CUL3 (CUL3Δ9) exhibit elevated RhoA/ROCK signaling in the vasculature and whether arterial stiffness is a hallmark in these patients.

Arterial stiffness is a predictor of human cardiovascular outcomes and end-organ damage (20), and increased PWV has been shown to precede the development of clinical hypertension (21). PWV was elevat-ed in S-CUL3Δ9 mice, and arterial compliance was decreased by subpressor dose of Ang II in these mice. Notably, smooth muscle–specific expression of CUL3Δ9 recapitulates alterations in arterial pulse wave-forms in mice expressing mutant CUL3 in all cells (6), suggesting this is a direct effect of CUL3 activity within vascular smooth muscle.

The renal tubule controls fluid and electrolyte homeostasis and consequently plays an important role in BP regulation (22). But our study raises important questions about the presumed mechanism of increased BP in PHAII and perhaps other forms of hypertension that are believed to be salt dependent. Our data suggest that increased vascular tone, perhaps including renal vascular tone, could play a role in the hypertension in PHAII patients with CUL3 mutations. Although we did not specifically measure renal vascular resistance in the S-CUL3Δ9 model, alterations in renal vascular tone were reported to have marked effects on total peripheral resistance and thus BP in humans (23). Similarly, other results support the concept that alterations in vascular smooth muscle can alter BP without changes in renal sodium handling. For example, deletion of the mineralocorticoid receptor in SMC in mice results in hypotension and protection from Ang II–induced pressor responses (24). Hypertension in apparent mineralocorticoid excess syndrome has been presumed to be caused by sodium retention in the distal nephron, but recent studies showed that deletion of the gene encoding 11β-hydroxysteroid dehydrogenase type 2 (11βHSD2) specifically in the brain caused increased salt sensitivity causing salt-sensitive hypertension independent of alterations in renal sodium excretion or fluid retention (25).
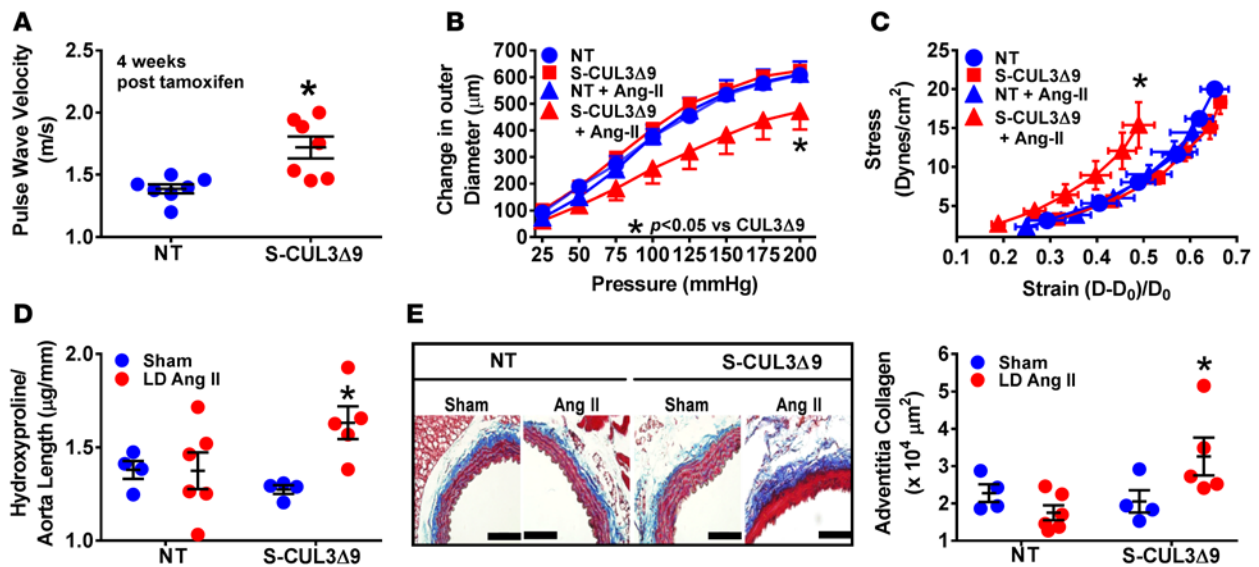
Figure 8. Aortic compliance in S-CUL3Δ9 mice. (**A**) Pulse wave velocity measurements in nontransgenic (NT) and S-CUL3Δ9 mice, as determined by Doppler ultrasound. $n = 7$/genotype. *$P < 0.05$ S-CUL3Δ9 vs. NT by 1-way ANOVA. (**B** and **C**) Pressure-diameter curves (**B**) and stress-strain relationships (**C**) of NT and S-CUL3Δ9 aortas. $n = 4$–6/genotype/treatment. *$P < 0.05$ angiotensin II (Ang II) S-CUL3Δ9 vs. all other curves by 1-way repeated-measure ANOVA. (**D**) Aortic collagen, as measured by hydroxyproline assay. $n = 4$–6/genotype/treatment. *$P < 0.05$ Ang II S-CUL3Δ9 vs. all other samples by 1-way ANOVA. (**E**) Adventitial collagen was determined by Masson trichrome staining. Original magnification, ×40; scale bar: 100 μm. $n = 4$–6/genotype/treatment. *$P < 0.05$ Ang II S-CUL3Δ9 vs. all other samples analyzed by 1-way ANOVA.

The phenotype in S-CUL3Δ9 mice described herein demonstrates a plausible vascular mechanism contributing, at least in part, to severe early-onset hypertension seen in PHAII patients. Increased vasoconstriction coupled with increased SBP could serve as a feed-forward mechanism, worsening arterial stiffness, hypertension, and end-organ damage with aging. These examples suggest that extratubular mechanisms of BP regulation in some inherited forms of Mendelian hypertension be considered.

Methods

See the Supplemental Experimental Methods for detailed methodology.

Animals. Mice inducibly expressing *CUL3Δ9* were generated at the University of Iowa Gene Editing Facility using vector designed to inducibly express any cDNA (26). The genetic background was C57BL/6 × B6SJL, with continuous backcross breeding to C57BL/6. *CUL3Δ9* transgenic mice were bred with mice expressing a tamoxifen-inducible Cre recombinase (CreERT²) under the control of the smooth muscle myosin heavy chain promoter (B6.FVB-Tg(Myh11-cre/ERT2)1Soff/J, Jax stock 019079). Tamoxifen was administered (75 mg/kg) i.p. daily for 5 consecutive days. Male age-matched S-CUL3Δ9 and NT littermate control mice were used. Male mice were used because the bacterial artificial chromosome transgene encoding inducible smooth muscle–specific Cre recombinase used in this study is inserted on the Y chromosome. Thus, only male mice inherit the transgene.

BP. BP was measured by radiotelemetry. Mice were implanted with an osmotic minipump (Alzet model 1002) to infuse Ang II (200 ng/kg/min) for 14 days. All data were collected and stored using Dataquest ART software.

Vascular function. Aortas were isolated, cleaned of adventitia fat, and suspended in an organ bath. Vascular reactivity experiments were conducted using a wire myograph as previously described (1). Cerebral basilar arteries were isolated and pressurized at 60 mmHg. Vascular function and vessel morphometry were determined using a Danish Myograph Technology system as previously reported (27).

PWV and stress strain analysis. PWV was measured using Doppler ultrasound (MouseDoppler, Indus Instruments) (28). Stress-strain studies using thoracic aortas were as previously described (29). Aortic collagen was measured by hydroxyproline assay. Adventitial collagen was stained, visualized using Masson's trichrome staining, and quantified by planimetry using ImageJ (NIH) software.

Statistics. All data are expressed as mean ± SEM. Data were analyzed using unpaired 2-tailed Student's

t test, 1-way ANOVA, or 2-way ANOVA (repeated measures when appropriate) using Tukey or Bonferroni post-hoc tests. $P \leq 0.05$ was considered statistically significant. Data were analyzed using Graphpad Prism (Graphpad Prism 6 or 7 software).

Study approval. All animal protocols were approved by the University of Iowa Animal Care and Use Committee (5021294, 5101531) and were performed in accordance with the standards set forth by the NIH *Guide for the Care and Use of Laboratory Animals* (National Academies Press. 2011.).

Author contributions

LNA generated the construct for the generation of CUL3Δ9 transgenic mice and performed most of the experiments. JW performed stress-strain experiments, CH performed some experiments on basilar arteries, and DRD performed surgeries to implant radiotelemetry devices. LNA, FWQ, and CDS conceived and supervised the project, performed data analysis, and wrote the manuscript. SCI performed critical preliminary experiments and data analysis leading to the concept tested in this paper. HLK performed data analysis. All authors analyzed the results and read and approved the final version of the manuscript.

Address correspondence to: Curt D. Sigmund, Department of Pharmacology, Roy J. and Lucille A. Carver College of Medicine, University of Iowa, 2-471B-1 BSB, Iowa City, Iowa 52242, USA. Phone: 319.335.7410; E-mail: curt-sigmund@uiowa.edu.

1. Pelham CJ, et al. Cullin-3 regulates vascular smooth muscle function and arterial blood pressure via PPARγ and RhoA/Rho-kinase. *Cell Metab*. 2012;16(4):462–472.
2. Boyden LM, et al. Mutations in kelch-like 3 and cullin 3 cause hypertension and electrolyte abnormalities. *Nature*. 2012;482(7383):98–102.
3. Furukawa M, He YJ, Borchers C, Xiong Y. Targeting of protein ubiquitination by BTB-Cullin 3-Roc1 ubiquitin ligases. *Nat Cell Biol*. 2003;5(11):1001–1007.
4. Ibeawuchi SR, Agbor LN, Quelle FW, Sigmund CD. Hypertension-causing mutations in Cullin3 protein impair RhoA protein ubiquitination and augment the association with substrate adaptors. *J Biol Chem*. 2015;290(31):19208–19217.
5. McCormick JA, et al. Hyperkalemic hypertension-associated cullin 3 promotes WNK signaling by degrading KLHL3. *J Clin Invest*. 2014;124(11):4723–4736.
6. Schumacher FR, et al. Characterisation of the Cullin-3 mutation that causes a severe form of familial hypertension and hyperkalaemia. *EMBO Mol Med*. 2015;7(10):1285–1306.
7. Wakabayashi M, et al. Impaired KLHL3-mediated ubiquitination of WNK4 causes human hypertension. *Cell Rep*. 2013;3(3):858–868.
8. Louis-Dit-Picard H, et al. KLHL3 mutations cause familial hyperkalemic hypertension by impairing ion transport in the distal nephron. *Nat Genet*. 2012;44(4):456–60, S1–3.
9. Wilson FH, et al. Human hypertension caused by mutations in WNK kinases. *Science*. 2001;293(5532):1107–1112.
10. Halabi CM, et al. Interference with PPAR gamma function in smooth muscle causes vascular dysfunction and hypertension. *Cell Metab*. 2008;7(3):215–226.
11. De Silva TM, et al. Role of peroxisome proliferator-activated receptor-γ in vascular muscle in the cerebral circulation. *Hypertension*. 2014;64(5):1088–1093.
12. Beltran A, et al. Arterial compliance abnormalities in isolated systolic hypertension. *Am J Hypertens*. 2001;14(10):1007–1011.
13. Singer JD, Gurian-West M, Clurman B, Roberts JM. Cullin-3 targets cyclin E for ubiquitination and controls S phase in mammalian cells. *Genes Dev*. 1999;13(18):2375–2387.
14. Ohh M, et al. An intact NEDD8 pathway is required for Cullin-dependent ubiquitylation in mammalian cells. *EMBO Rep*. 2002;3(2):177–182.
15. Shimokawa H, Sunamura S, Satoh K. RhoA/Rho-kinase in the cardiovascular system. *Circ Res*. 2016;118(2):352–366.

16. Kitazawa T, Gaylinn BD, Denney GH, Somlyo AP. G-protein-mediated Ca2+ sensitization of smooth muscle contraction through myosin light chain phosphorylation. *J Biol Chem*. 1991;266(3):1708–1715.

17. Sakurada S, et al. Ca2+-dependent activation of Rho and Rho kinase in membrane depolarization-induced and receptor stimulation-induced vascular smooth muscle contraction. *Circ Res*. 2003;93(6):548–556.

18. Chen Y, et al. Cullin mediates degradation of RhoA through evolutionarily conserved BTB adaptors to control actin cytoskeleton structure and cell movement. *Mol Cell*. 2009;35(6):841–855.

19. Leck YC, Choo YY, Tan CY, Smith PG, Hagen T. Biochemical and cellular effects of inhibiting Nedd8 conjugation. *Biochem Biophys Res Commun*. 2010;398(3):588–593.

20. Laurent S, et al. Aortic stiffness is an independent predictor of all-cause and cardiovascular mortality in hypertensive patients. *Hypertension*. 2001;37(5):1236–1241.

21. Kaess BM, et al. Aortic stiffness, blood pressure progression, and incident hypertension. *JAMA*. 2012;308(9):875–881.

22. Chen D, Coffman TM. The kidney and hypertension: lessons from mouse models. *Can J Cardiol*. 2012;28(3):305–310.

23. Damkjaer M, et al. Selective renal vasoconstriction, exaggerated natriuresis and excretion rates of exosomic proteins in essential hypertension. *Acta Physiol (Oxf)*. 2014;212(1):106–118.

24. McCurley A, et al. Direct regulation of blood pressure by smooth muscle cell mineralocorticoid receptors. *Nat Med*. 2012;18(9):1429–1433.

25. Evans LC, et al. Conditional Deletion of Hsd11b2 in the Brain Causes Salt Appetite and Hypertension. *Circulation*. 2016;133(14):1360–1370.

26. Stump M, et al. Effect of selective expression of dominant-negative PPARγ in pro-opiomelanocortin neurons on the control of energy balance. *Physiol Genomics*. 2016;48(7):491–501.

27. Hu C, Lu KT, Mukohda M, Davis DR, Faraci FM, Sigmund CD. Interference with PPARγ in endothelium accelerates angiotensin II-induced endothelial dysfunction. *Physiol Genomics*. 2016;48(2):124–134.

28. Hartley CJ, Taffet GE, Reddy AK, Entman ML, Michael LH. Noninvasive cardiovascular phenotyping in mice. *ILAR J*. 2002;43(3):147–158.

29. Wu J, et al. Inflammation and mechanical stretch promote aortic stiffening in hypertension through activation of p38 mitogen-activated protein kinase. *Circ Res*. 2014;114(4):616–625.

30. Stump M, et al. Nervous System Expression of PPARγ and Mutant PPARγ Has Profound Effects on Metabolic Regulation and Brain Development. *Endocrinology*. 2016;157(11):4266–4275.